This article was downloaded by:
On: *22 January 2011*
Access details: *Access Details: Free Access*
Publisher *Taylor & Francis*
Informa Ltd Registered in England and Wales Registered Number: 1072954 Registered office: Mortimer House, 37-41 Mortimer Street, London W1T 3JH, UK

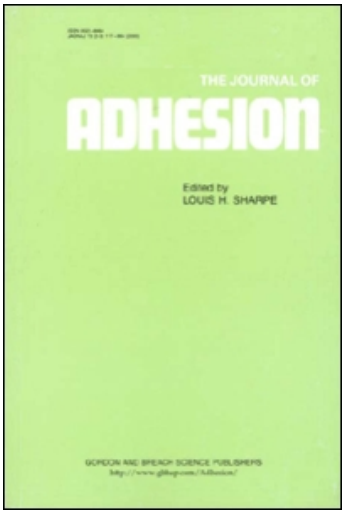

The Journal of Adhesion
Publication details, including instructions for authors and subscription information:
http://www.informaworld.com/smpp/title~content=t713453635

The Adhesion of Maleic Anhydride on Native Aluminum Oxide: An Approach by Infrared Spectroscopy and Quantum Mechanical Modeling

Bernhard Schneider[a]; Otto-Diedrich Hennemann[a]; Wulff Possart[b]
[a] Fraunhofer Institute of Applied Materials Research, Bremen, Germany [b] Saarland University, Saarbruecken, Germany

Online publication date: 08 September 2010

To cite this Article Schneider, Bernhard , Hennemann, Otto-Diedrich and Possart, Wulff(2002) 'The Adhesion of Maleic Anhydride on Native Aluminum Oxide: An Approach by Infrared Spectroscopy and Quantum Mechanical Modeling', The Journal of Adhesion, 78: 9, 779 — 797
To link to this Article: DOI: 10.1080/00218460213837
URL: http://dx.doi.org/10.1080/00218460213837

PLEASE SCROLL DOWN FOR ARTICLE

Full terms and conditions of use: http://www.informaworld.com/terms-and-conditions-of-access.pdf

This article may be used for research, teaching and private study purposes. Any substantial or systematic reproduction, re-distribution, re-selling, loan or sub-licensing, systematic supply or distribution in any form to anyone is expressly forbidden.

The publisher does not give any warranty express or implied or make any representation that the contents will be complete or accurate or up to date. The accuracy of any instructions, formulae and drug doses should be independently verified with primary sources. The publisher shall not be liable for any loss, actions, claims, proceedings, demand or costs or damages whatsoever or howsoever caused arising directly or indirectly in connection with or arising out of the use of this material.

The Journal of Adhesion, 78: 779–797, 2002
Copyright © 2002 Taylor & Francis
0021-8464/02 $12.00 +.00
DOI:10.1080/00218460290010511

Downloaded At: 09:21 22 January 2011

THE ADHESION OF MALEIC ANHYDRIDE ON NATIVE ALUMINUM OXIDE: AN APPROACH BY INFRARED SPECTROSCOPY AND QUANTUM MECHANICAL MODELING

Bernhard Schneider
Otto-Diedrich Hennemann
Fraunhofer Institute of Applied Materials Research, Bremen, Germany

Wulff Possart
Saarland University, Saarbruecken, Germany

The bonding between maleic anhydride, a curing agent for epoxy resins, and natively oxidized aluminum is studied by a combination of infrared spectroscopy and quantum mechanical modeling. On native aluminum oxide, maleic anhydride is hydrolyzed to maleic acid in the early stages of adhesion. The acid prefers a bridged chelate bond of one of its acid groups to two Al atoms of the metal oxide. Furthermore, a monodentate bond between a carbonyl oxygen of an acid group and an Al atom is identified. The anhydride itself shows no tendency to adhere on the native aluminum oxide. Since maleic acid is less reactive in the polymerization than the anhydride, the results imply that the chemical curing reaction could be hampered in the vicinity of the Al substrate.

Keywords: Molecular modeling; Density functional theory; Chemical adhesion; Maleic anhydride; Maleic acid; Aluminum oxide

INTRODUCTION

The relationship between the composition of an adhesive joint and its properties depends on its microscopic structure. On this scale, the interphase plays an important role [1]. The development of the

Received 15 November 2001; in final form 10 April 2002.
Presented in part at the 24th Annual Meeting of The Adhesion Society, Inc., held in Williamsburg, Virginia, USA, 25–28 February 2001.
Address correspondence to Wulff Possart, Saarland University, P.O.B. 151150, D-66041 Saarbruecken, Germany. E-mail: w.possart@mx.uni-saarland.de

interphase can commence with the application of the adhesive in its initial liquid state on the substrates to be joined. For example, if the curing agent of a network-forming adhesive interacts strongly with the substrate surface, the affected molecules cannot participate properly in the chemical curing reaction near the surface, and the network of the cured adhesive possesses a different structure in this region from that in the bulk phase. The study of the interaction of single adhesive components with the substrate surface provides a first step towards the understanding of the development of the interphase.

In this paper, the type of bonding between maleic anhydride (a curing agent for epoxy resins) and natively oxidized aluminum will be elucidated. The task is approached by combining infrared external reflection absorption spectroscopy (ERAS) and quantum mechanical modeling. Infrared spectroscopy is widely applied in adhesion science (e.g., [2, 3]), and quantum mechanical modeling as well has been used for identifying the nature of adhesive bonding [4]. The combination of both is rare but not entirely new in adhesion science (e.g., [5]). However, the program codes and hardware capacity of today allow a more sophisticated treatment of problems related to adhesion than a couple of years ago. In this paper, quantum mechanical calculations will be applied not only for the modeling of electronic structures but also for the calculation of the corresponding infrared spectra.

Downloaded At: 09:21 22 January 2011

SAMPLE PREPARATION AND EXPERIMENTAL METHODS

Polished silicon wafers with an evaporated layer of pure aluminum (99.999%, from Balzers, $d_{Al} > 500\,nm$ according to Tolanski interference microscopy) provide the very smooth substrate that is essential for infrared external reflection spectra of high quality. After electron beam evaporation (base pressure 2×10^{-6} Pa), the polycrystalline Al surface is brought into contact with pure oxygen in order to create a uniform layer of amorphous oxide as was shown by in situ X-ray Photoelectron Spectroscopy. Then, the substrate is transferred into laboratory atmosphere where the surface composition is completed by the adsorption of water and of the usual organic contaminants as revealed by XPS. After 4 weeks of storage time in laboratory atmosphere, the substrate surface has reached equilibrium. According to variable angle spectroscopic ellipsometry (Woollam M44, angle of incidence 65–85°, 414–747 nm), the total layer thickness on the Al is found to be between 3.9–4.8 nm, depending on the sample history. Atomic Force Microscopy (AFM) (Nanoscope III Dimension 3000, contact mode) depicts the surface topography with a mean

square roughness of about 1.5 nm and inclination angles around 6° for the surface facets.

The maleic anhydride is deposited in the monolayer range on this well-controlled surface. A fresh solution of 5 mass% maleic anhydride (Aldrich, 99 +%) in acetone (Aldrich, 99.9 +%, for high pressure liquid chromatography) is utilized for spin coating (5 s at 5000 rpm). Within some 30 s after spinning, the originally white coating disappears and the substrate surface seems to be clean because most of the deposited anhydride evaporates quickly. Ellipsometric analysis confirms that the residual organic layer is less than 1 nm thick.

IR external reflection spectra (2000 scans, spectral resolution $2\,cm^{-1}$) are recorded for such residual organic layers with p-polarized light on a Harrick Seagull reflection unit at 80° angle of incidence in the evacuated sample compartment (200 Pa) of a Bruker IFS 66v equipped with a MCT detector. The principle of external reflection absorption spectroscopy (ERAS) is sketched briefly in Figure 1.

Downloaded At: 09:21 22 January 2011

The incident light has to be polarized linearly (parallel (p) or perpendicularly (s) with respect to the plane of incidence). It penetrates the thin organic layer on the plane substrate mirror, thus causing a sequence of multiple reflections and refractions as well as absorption by the materials. Accordingly, the leaving beams possess a phase shift that results in interference depending on wavelength, angle of incidence, film thickness, and optical functions $\hat{n}(\tilde{\nu}) = n(\tilde{\nu}) - i \cdot k(\tilde{\nu})$ of the film, the substrate, and the surrounding medium. The interference pattern is recorded as the IR reflection spectrum at the detector.

For comparison, IR transmission spectra are measured for maleic anhydride and for maleic acid in KBr pellets in dry air in the same spectrometer.

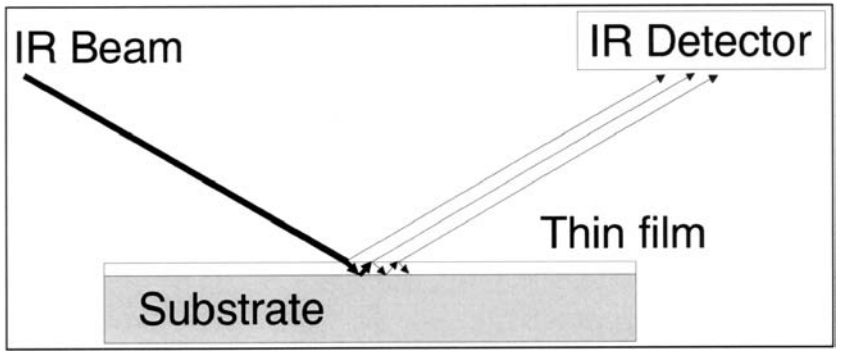

FIGURE 1 Sketch of the measuring principle of external reflection absorption spectroscopy.

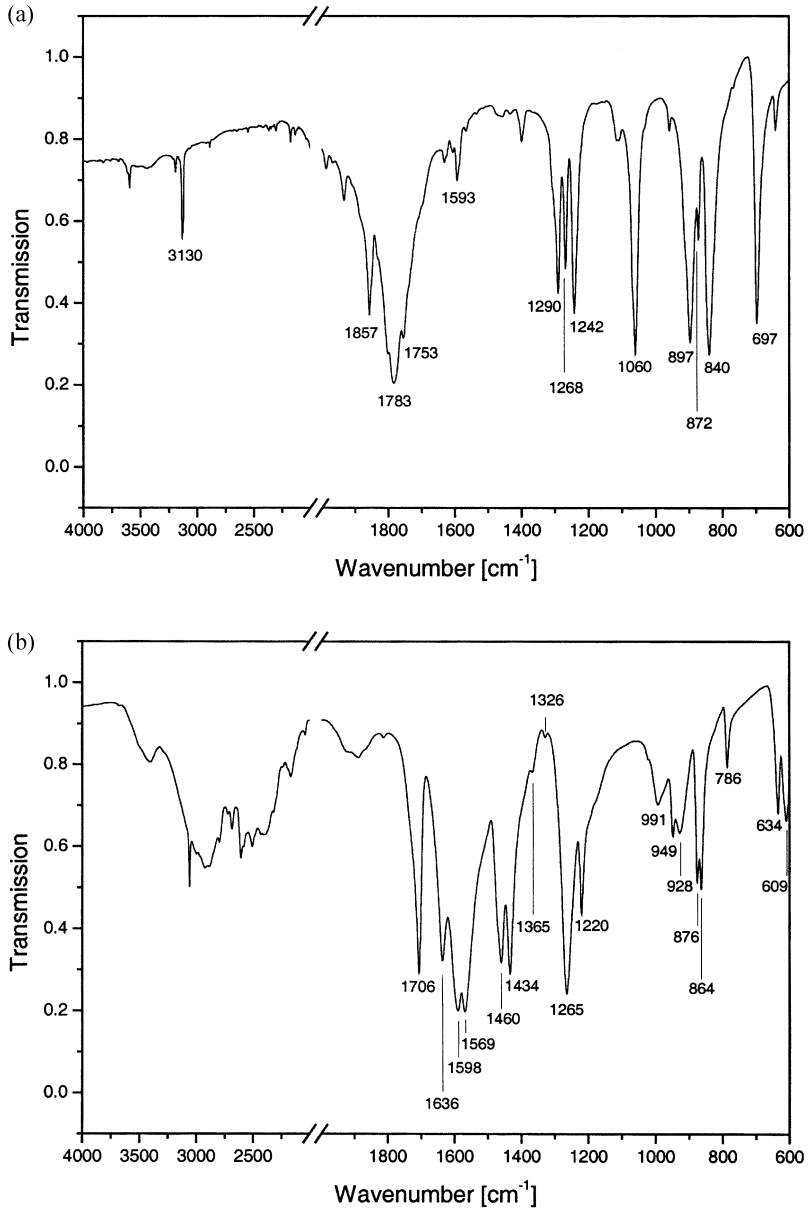

Downloaded At: 09:21 22 January 2011

FIGURE 2 Infrared transmission spectra of maleic anhydride (a) and maleic acid (b). The transmission T is calculated by $T = I(\text{sample})/\ I(\text{background})$ from the single beam IR spectra that are measured for KBr plates with epoxy (I (sample)) and without epoxy (I (background)).

IR-SPECTROSCOPY: RESULTS

Figure 2 presents the transmission spectra for maleic anhydride and maleic acid in KBr pellets (bulk state). The two spectra differ very clearly in the spectral range shown.

For convenience, the chemical formulae are given (Scheme 1):

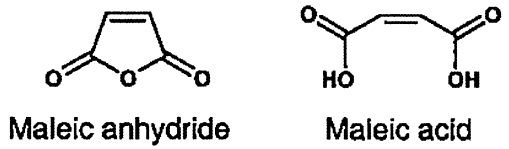

SCHEME 1

An approximate assignment of the most characteristic absorption bands is given in Table 1 for the anhydride and the acid, respectively.

Downloaded At: 09:21 22 January 2011

TABLE 1 Characteristic IR Absorption Bands for Maleic Anhydride and for Maleic Acid According to Schneider [6]

Maleic anhydride		Maleic acid	
Band positions [cm^{-1}]	Approximate assignment	Band positions [cm^{-1}]	Approximate assignment
1857	C=O symmetr. stretch		
1783	C=O asymmetr. stretch		
		1706	C=O stretch
		1636	C=C & C=O stretch
1593	C=C stretch	1598	C=O & C=C stretch
		1569	C=O & C=C stretch
		1460	O–H deformation
		1434	O–H deformation
1290	C–O–C deformation	1265	C–OH stretch & C–H deformation
1268	O–C=O deformation & ring deformation		
1242	C–O–C symmetr. stretch	1220	C–OH stretch
1060	in-plane ring vibration		
897	O=C–O–C=O asymmetr. deformation		
		876	C–H out-of-plane deformation
		864	C–H out-of-plane deformation
872	O=C–O–C=O asymmetric deformation		
840	out-of-plane ring vibration		
697	in-plane ring vibration		

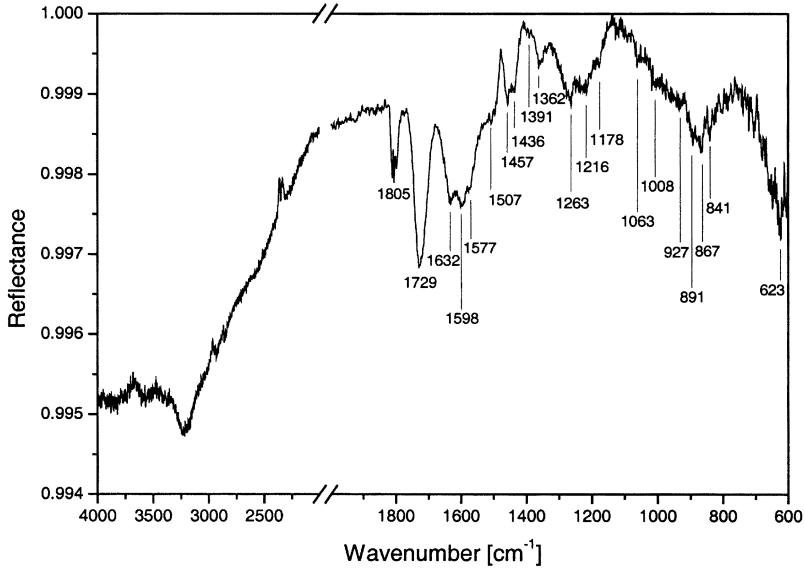

FIGURE 3 A natively oxidized aluminum substrate coated with an extremely thin layer of maleic anhydride. ERA spectrum taken after about 1 min exposure to laboratory atmosphere.

Downloaded At: 09:21 22 January 2011

Figure 3 provides the ERA spectrum of a freshly-prepared, ultrathin film on the aluminum substrate after spin coating with the above-mentioned anhydride solution. All reflectance spectra are obtained from

$$R = \frac{I\ (\text{sample})}{I\ (\text{background})},$$

with the single-beam IR spectra measured on the aluminum substrate prior (I (background)) and after spin coating (I (sample)). The very weak bands in the reflectance spectrum confirm that the organic coating is extremely thin.

A quick qualitative inspection reveals that the ERA spectrum in Figure 3 resembles rather the spectrum of the acid than the spectrum of the anhydride (compared with both spectra in Figure 2). As was shown in additional experiments [6], the triplet band around 1805 cm^{-1} is caused by gaseous maleic anhydride that has been evaporated from the specimen into the sample compartment of the spectrometer. Probably the IR absorptions at 1063 cm^{-1}, 891 cm^{-1}, and

TABLE 2 Prominent Infrared Absorption Bands of Maleic Acid in Bulk (KBr Pellet) Compared with the ERAS Bands of a Freshly Prepared, Ultrathin Film of the Maleic Anhydride on Native Al Oxide

Maleic acid in KBr pellet		ERAS of the maleic anhydride film	
Band positions [cm^{-1}]	Approximate assignment	Band positions [cm^{-1}]	Approximate assignment
		1805	Gaseous maleic anhydride
1706	C=O stretch	1729	C=O stretch in maleic acid[a]
1636	C=O & C=C stretch	1632	C=C stretch in adsorbed maleate[a]
1598	C=C & C=O stretch	1598	?
1569	C=C & C=O stretch	1577	O–C–O asymmetr. stretch in adsorbed maleate[a]
1460	O–H deformation	1457	O–C–O symmetr. stretch in adsorbed maleate[a]
1434	O–H deformation	1436	?
		1362	C–O stretch in maleate[a]
1265	C–OH stretch	1263	C–O–C stretch in adsorbed maleic anhydride[a]
1220	C–OH stretch	1216	?
		1178	?
		1063	Gaseous maleic anhydride
876	C–H deformation	891	Gaseous maleic anhydride
864	C–H deformation	867	?
		841	Gaseous maleic anhydride

[a] Assignment according to the proposal of Do and Baerns [7].

Downloaded At: 09:21 22 January 2011

841 cm^{-1} also result, at least in part, from this anhydride vapor. The majority of the remaining IR bands in the ERA spectrum match well with the infrared bands of maleic acid—see Table 2. We conclude that the surface of the native aluminum oxide stimulates the hydrolysis of the anhydride into maleic acid, which is capable of adsorbing on the substrate. Either the humid atmosphere or the native adsorption layer on the oxide can supply the necessary water or hydroxyl groups. Hydrolysis and adsorption agree well with conclusions drawn by other researchers on the adsorption behavior of anhydrides on metal oxides [7, 8].

Several authors (e.g., [7–10]) take the small differences in the band positions of bulk and adsorbed maleic acid (see Table 2) for an indication that the acid is chemisorbed. Generally, such conclusions may not be derived directly from ERA spectra for the following reasons. First, band positions and intensity distribution of reflection spectra from thin films result not only from the absorption of light by the molecules in the film but also from the superimposed

interference patterns that are produced by multiple reflections/refraction of light at the film surface and at the interface with the substrate (see, e.g., [11, 12, 13]). Any additional structure in the film (islands, porosity, structure gradients, etc.) will add further complications. Secondly, the orientation of the adsorbed molecules with respect to the surface normal of the metal substrate brings the so-called surface selection rule into effect: molecular vibration modes are able to absorb energy from the incoming light only if they possess a component of the transition dipole moment that is perpendicular to the metal surface.

Accordingly, the comparison of ERA spectra with catalogues of IR spectra or with bulk spectra does not provide reliable arguments for conclusions on the chemical adhesion of adhesive molecules on solids. Therefore, we will solve this problem by simulating the spectra for a variety of plausible geometric arrangements of adsorbed maleic acid on aluminum oxide surface clusters. Quantum mechanical calculations provide the basis for this simulation.

Downloaded At: 09:21 22 January 2011

QUANTUM MECHANICAL CALCULATIONS: ADHESION MODELS AND SIMULATED ERA SPECTRA

As shown above, the experimental results indicate that the maleic anhydride is hydrolyzed to maleic acid. Therefore, in the model calculations the adhesion of the acid is considered.

According to the literature, the oxide layer on natively oxidized aluminum consists of amorphous γ-alumina [14–18]. The Al atoms are tetrahedrally or octahedrally surrounded by oxygen atoms [16, 19–21]. The surface is covered with chemisorbed and physisorbed water [22, 23]. Aluminum ions exposed to the oxide surface are expected to provide the most reactive surface sites [24].

The density functional program DMol (Vers. 4.0.0, MSI Inc., San Diego, California) is utilized for the quantum mechanical modeling of different adhesion states of the maleic acid molecule on native aluminum oxide. A quantum mechanical approach is inevitable for our purposes. A priori, all less sophisticated levels of modeling such as molecular mechanics with force fields or a semiempirical approach cannot account for appearing interactions. The energy minimum of adsorbate/substrate configurations is calculated very precisely in order to gain reliable frequency values for the eigenvibrations of each configuration.

Cluster models have to be used for the quantum mechanical modeling of solid surfaces because the number of atoms (i.e., the number of electron wave functions) is limited, mainly due to computing time. The

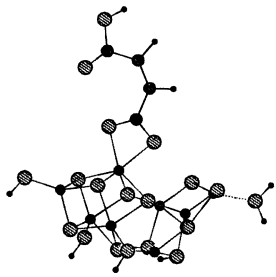

H
C
O
Al

1 chelate bond to octahedral Al

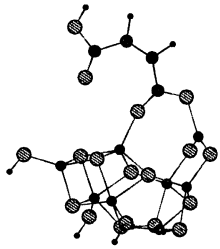

2 bridged chelate bond to octahedral and tetrahedral Al

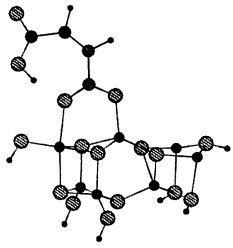

3 bridged chelate bond to octahedral and tetrahedral Al with intramolecular hydrogen bond

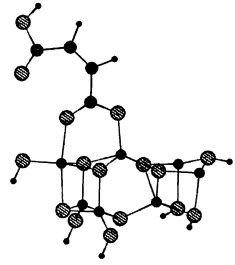

4 bridged chelate bond to octahedral and tetrahedral Al

FIGURE 4 Adhesive-cluster models, Part I: The native aluminum oxide is represented by cluster models. The hydrolyzed maleic anhydride (i.e., maleic acid) is bonded in different ways on top of the oxide.

cluster models used in this work account for the local structure of the amorphous oxide. They contain tetrahedrally and octahedrally coordinated Al surface sites. From the numerical point of view, these clusters consist of quite a large number of atoms.

Downloaded At: 09:21 22 January 2011

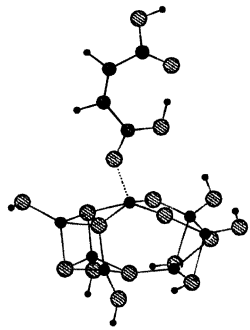

5 monodentate bond to a octahedral Al with intermolecular hydrogen bond

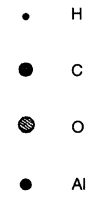

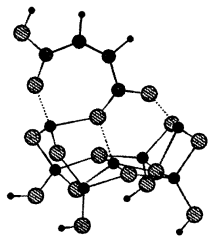

6 chelate bond via two acid groups to two tetrahedral Al

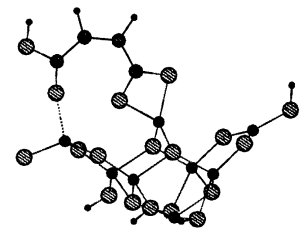

7 chelate bond to a tetrahedral Al with a coordinative carbonyl Al bond

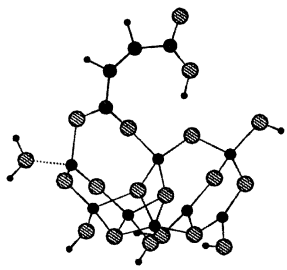

8 bridged chelate bond to two tetrahedral Al with hydrogen bond to the surface

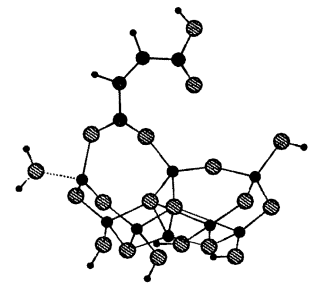

9 bridged chelate bond to two tetrahedral Al

FIGURE 5 Adhesive-cluster models, Part II: The native aluminum oxide is represented by cluster models. The hydrolyzed maleic anhydride (i.e., maleic acid) is bonded in different ways on top of the oxide.

Downloaded At: 09:21 22 January 2011

We designed quite a number of cluster models that represent chemically plausible types of bonding of maleic acid to the substrate surface. Nine of them are depicted in Figures 4 and 5.

In accordance with assumptions in the literature [7, 8, 25] about the bonding of carboxylic acids to metal oxides, we consider bonds of one or two of the acid groups and Al ions in tetrahedral or octahedral oxygen coordination. Since the aluminum surface sites are very reactive they are occupied by water or other adsorbates. The maleic acid groups only get access to these sites due to a chemical reaction like the hydrolysis of maleic anhydride or the competitive adsorption between the adsorbed species and maleic acid. All cluster configurations shown in Figures 4 and 5 are in equilibrium, i.e., they reached a well-calculated minimum of electronic energy. In some cases, the acid-substrate bonds possess a chelate-like character. In several cases, additional hydrogen bonds are involved, both as intramolecular bonds or with the surface.

Downloaded At: 09:21 22 January 2011

For each energy-optimized, adhesive-cluster model, the normal modes of vibration (i.e., their frequency and transition dipole moment vector) are calculated. Eigenfrequency data obtained with density functional algorithms are known for their good accuracy as compared with other ab initio algorithms [26–29]. This was also validated in [6] with DMol for a number of organic compounds: anhydrides, carboxylic acids, alkenes, and ketones. It turns out that DMol overestimates CH_n stretch vibrations by about $50-100\,cm^{-1}$. The OH stretch vibrations are underestimated by ca. $50\,cm^{-1}$. All calculated frequencies of normal vibrations in the range below $2500\,cm^{-1}$ are mostly too low by about $25\,cm^{-1}$. The transition dipole moment vectors are reliable with respect to the orientation in the molecule. Their absolute values, which are related to the intensity of the corresponding bands of light absorption, are less accurate. They can be used in a qualitative manner, i.e., big transition dipole moments correspond to strong bands and small moments to weak bands, but the ranking of the dipolar strengths does not match very well to the intensity ratios in measured IR spectra [30].

With the calculated data for the normal vibration modes, the IR reflection spectra can now be simulated as they would be measured by ERAS in the case that the considered adsorbate/cluster configuration would exist at surface sites on the native aluminum oxide. For these simulations, only those vibrations are selected from the complete set of normal modes that include appreciable motions of atoms in the adsorbed organic molecule. Every vibration is described by a frequency and by a transition dipole moment $\vec{\mu}^{trans}$ of a certain orientation with respect to the cluster surface. For the simulated ERA spectrum, each

infrared active mode is represented by a Gaussian line shape with an arbitrarily chosen line width. This produces just the usual look for the spectra. The intensity I of an IR band is given by

$$I \propto |\vec{E}_0^{\text{light}} \cdot \vec{\mu}^{\text{trans}}|^2,$$

where $\vec{E}_0^{\text{light}}$ = electric field strength amplitude of the light. Hence, the peak height (i.e., the intensity) of each Gaussian line is set proportional to the square of the normal component (z-direction) of $\vec{\mu}^{\text{trans}}$ on the aluminum surface,

$$I^{\text{ERAS}} \propto (\vec{\mu}_z^{\text{trans}})^2,$$

thus taking the surface selection rule into account. The simulated ERA spectra for the considered nine adsorbate/cluster arrangements are shown in Figure 6.

It is important to note that all spectra are easy to distinguish from each other. Therefore, every spectrum is characteristic for a particular kind of bonding between maleic acid and aluminum oxide, and we are

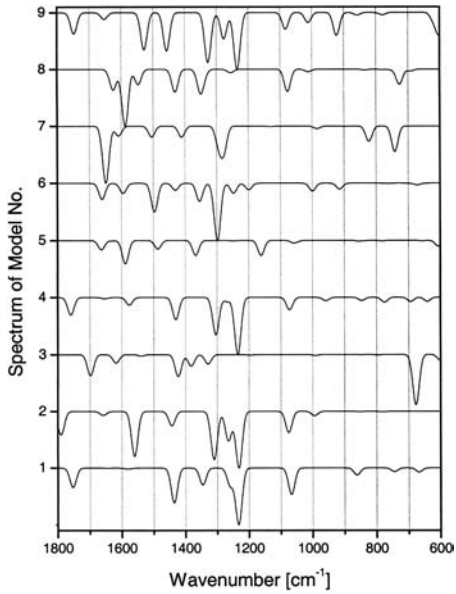

FIGURE 6 Simulated ERA spectra for the considered adhesive-cluster models. On the ordinate, each spectrum is marked with the number of the corresponding adhesive-cluster model given in Figures 4 and 5. For all spectra, the intensity of the strongest band is scaled to the same value.

Downloaded At: 09:21 22 January 2011

able to identify the type of bonding by comparing a measured ERA spectrum with the simulated spectra in Figure 6.

CORRELATION BETWEEN MEASURED AND SIMULATED ERA SPECTRA

It was shown by Schneider [6] that the slight surface roughness of the aluminum substrate does not seriously affect the measured ERA spectra. Therefore, the spectrum in Figure 3 can be directly compared with the simulated ERA spectra in Figure 6. It is easy to establish that any single simulated spectrum is not sufficient to cover the experimental spectrum well. It is not imperative to use only one simulated spectrum: however, since the maleic acid could adsorb in several states as the real oxide surface offers many sites of different structure and reactivity. A careful consideration reveals that the spectrum of the real sample contains all absorption bands of only the simulated spectra Nos. 3, 5, and 8 in Figure 6 (the corresponding adhesive-cluster models are given in Figures 4 and 5). All possible combinations of the other simulated spectra are found to be lacking since they contain bands that do not appear in the ERA spectrum. Table 3 compares the band positions of the measured spectrum with the selected three simulated spectra and provides the assignment according to the calculated eigenvibrations. Mostly, the calculated wavenumbers are about $10-40\,\mathrm{cm}^{-1}$ lower than the experimental data. According to the above section, "Quantum Mechanical Calculations," DMol calculations tend to underestimate the frequency of most normal modes in the considered spectral region. Therefore, this set of simulated spectra is well suited to describe the real ERA spectrum of adsorbed maleic anhydride on native aluminum oxide. As shown in Figure 7, a weighted sum of these three spectra

$$\mathbf{6} \cdot \text{spectrum(No. } \mathbf{3}\text{)} + \mathbf{1} \cdot \text{spectrum(No. } \mathbf{5}\text{)} + \mathbf{1} \cdot \text{spectrum(No. } \mathbf{8}\text{)}$$

fits the measured spectrum in a reasonable way.

It was mentioned in the above section, "Quantum Mechanical Calculations," that the band intensities are obtained from DMol with a considerable error. The weight factors in the superposition cannot correct the approximative character of the intensity of a calculated spectrum. Therefore, it makes no sense to spend too much effort on their calculation. They were estimated simply by adjusting them on values that give a good visual agreement between fit and measured spectrum in Figure 7. Within these limits, the weight factors indicate roughly how often the different adsorption states occur on the aluminum oxide.

Downloaded At: 09:21 22 January 2011

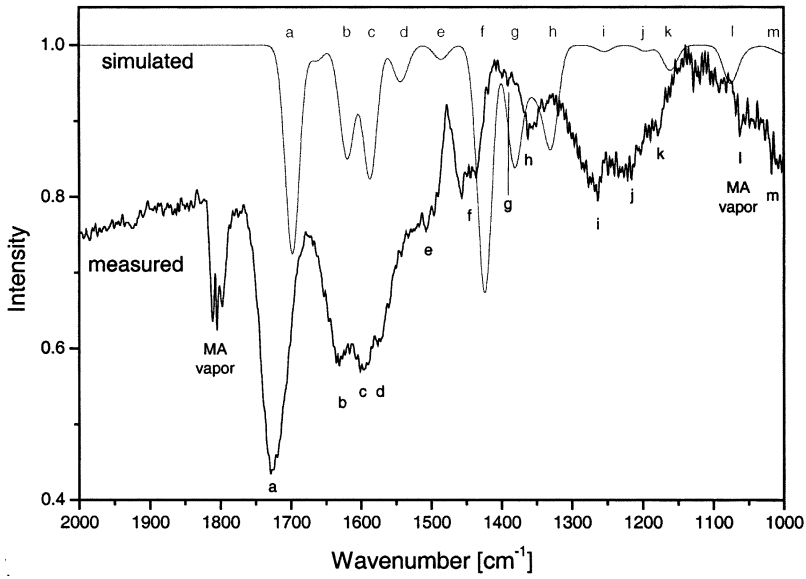

FIGURE 7 Real ERA spectrum of maleic anhydride adsorbed on the native oxide of pure aluminum (shifted downwards for clarity) and the weighted sum of the spectra simulated for adhesive-cluster models Nos. **3**, **5**, and **8**. The small letters at the bands help to correlate the measured and the simulated spectra.

Downloaded At: 09:21 22 January 2011

The band assignments in Table 3 offer additional insight into the nature of the adsorption states of the adsorbed maleic acid. Aside from the bands ***e***, ***j***, and ***k***, all other infrared bands in the ERA spectrum contain contributions from normal modes of two or of all three adhesive-cluster configurations. The eigenvibrations of the non-adsorbed acid group in the different clusters contribute to the bands ***a***, ***c***, ***g***, ***h***, and ***j***–***l***. The adsorbed acid/carboxylate groups are involved in bands ***a*** and ***c***–***f***. This result illustrates very well that the bands of such IR spectra almost never can be attributed to single, localized eigenvibrations of the adsorbed species. One has to be careful with the assignment of the IR bands of adsorbed molecules. It can be misleading to consider them on the basis of common data for IR spectra of bulk samples.

The transition dipole moments provide another valuable source of information. For example, IR band ***a*** contains the stretching vibration of the free carbonyl in model 3 and the combined stretching of C = C and of the adsorbed C=O in model 5. It does not belong to the stretching vibration of the nonbonded acid as one might have expected

Downloaded At: 09:21 22 January 2011

TABLE 3 Band Positions [cm^{-1}] of the Measured ERA Spectrum of Maleic Anhydride on Native Aluminum Oxide and the Simulated ERA Spectra for the Adhesive-Cluster Models Nos. **3**, **5**, and **8** (see Figures 4 and 5)

	ERAS of real sample	Model no. **3**	Approx. assignment	Abs. values z-comp. of TDM	Model no. **5**	Approx. assignment	Abs. values z-comp. of TDM	Model no. **8**	Approx. assignment	Abs. values z-comp. of TDM
a	1729	1699	ν(C=O)	0.53/0.46	1665	**ν(C=O)** + ν(C=C)	0.45/0.44	—		
b	1632	1618	ν(C=C)	0.36/0.29	1631	ν(C=O) + ν(C=C)	0.42/0.03	1624	ν(C=C)	0.83/0.55
c	1598	—			1588	**ν(C=O)** + ν(C=C)	0.68/0.67	1586	ν(C=O) + **ν(OCO)>$_{as}$**	0.72/0.67
d	1577	1539	**ν(OCO)$_{as}$**	0.58/0.17	—			1546	**ν(OCO)$_{as}$** + ν(C=O)	0.60/0.35
e	1507	—			1486	**δ(OH)** + **ν(OCO)$_{as}$**	0.59/0.46	—		
f	1457/ 1436[a]	1423	**ν(OCO)$_s$** + δ(C–H)	0.54/0.47	—			1429	**ν(OCO)$_s$**	0.51/0.42
g	1391	1383	δ(OH)	0.39/0.37	1367	δ(OH) + ν(OCO)$_s$	0.55/0.54	—		
h	1362	1329	ν(OCO)$_s$ + δ(C–H)	0.55/0.28	—			1348	ν(OCO)$_s$	0.50/0.42
i	1263	1290	δ(C–H) + δ(O–H)	0.04/0.02	1249	δ(C–H)	0.13/0.09	1254	δ(C–H)	0.51/0.17
j	1216	1198	ν(C–OH)	0.23/0.10	—			—		
k	1178	—			1161	ν(C–OH)	0.58/0.57	—		
l	1063	—			1056	not local	0.26 /0.22	1075	δ(O–H)	0.71/0.42
m	1008	992	γ(C–H)	0.11/ 0.10	—			1011	not local	0.18/0.14

An approximate assignment of the calculated bands is given, as well as the corresponding absolute values (in arbitrary units) of the calculated transition dipole moments (TDM) and of their ERAS active z-components. Bold printed assignments refer to the acid group that is bonded to the surface. Mode symbols: ν_s, symmetric stretch; ν_{as}, asymmetric stretch; δ, in-plane deformation; γ, out-of-plane deformation.

[a] Here, residual water vapor causes the apparent band splitting. It is very likely that band ***f*** is a single band in reality, with a wave number between 1457 cm^{-1} and 1436 cm^{-1}.

from the bulk data (comp. Tables 1 and 2). Both modes possess fairly strong transition dipole moments (TDM) of 0.53 and 0.45 (in arbitrary units). Their z-components are almost equal. Thus, these vibrations contribute equally to the intensity of IR band ***a***. The z-components are also smaller than the absolute values of the TDM. Therefore, we see that the free carbonyl stretch in model 3 is inclined by about 30° with respect to the oxide surface normal. The combined stretching vibration is almost perpendicular (12°) to the oxide surface.

From the modeling point of view (Table 3), the nonbonded carboxylic acid groups can be assessed almost directly by the IR bands ***j*** (model 3) and ***k*** (model 5). A glance at the measured spectrum (Figure 7) teaches, however, that the bands in this spectral region are not well separated. Here, we profit from the modeling again. The data for the TDM and their z-components tell us that the C-OH bond in the nonbonded acid of model 3 deviates by 64° from the perpendicular orientation, while the same bond in model 5 is inclined by only 11°. All these inclination angles specify the orientation of the free acid groups with respect to the surface. These details are important for a possible reaction with other molecules such as epoxies.

The bonded carboxylate (models 3 and 8) has to be attributed to IR bands ***d*** (asymmetric stretch) and ***f*** (symmetric stretch). The adsorbed acid group (model 5) gives rise to its special IR band ***e***, which is difficult to relate to an orientation in space because it is a combination of stretch and deformation. Band ***d*** is dominated by model 8 but the TDM deviate considerably from the normal direction in both models. From band ***f*** we see that the plane of the bonded O-C-O is inclined by ca. 30° and 34° in models 3 and 8, respectively.

Of course, all such details of orientation can be obtained directly and more comfortably from the spatial models of the adhesive-cluster configurations in the computer.

CONCLUSIONS

The combination of infrared spectroscopy and quantum mechanical modeling provides access to a detailed understanding of the ERA spectrum that has been measured for an organic coating in the thickness range of a monolayer. The reasonable agreement of the measured and the simulated positions of IR bands supports the following conclusions on the adhesion mechanisms in the system.

After the coating of the natively oxidized aluminum substrate with a maleic anhydride solution, part of the anhydride is immediately hydrolyzed to maleic acid. This result confirms previous assumptions in the literature. It is not yet clear whether the water needed for the hydro-

Downloaded At: 09:21 22 January 2011

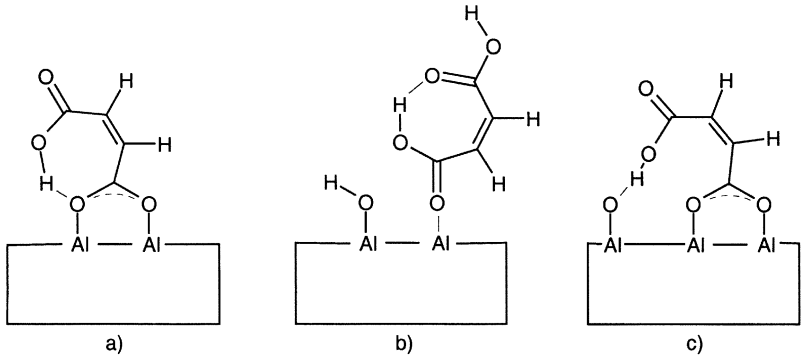

FIGURE 8 Schematic description of the bonds between maleic acid and aluminum surface sites on the native oxide of pure aluminum. Deduced from FTIR-ERAS and quantum chemical molecular modeling (density functional program DMol). (a) Bridged chelate bond of maleic acid with the native oxide according to the adhesive-cluster model No. **3**. The aluminum cations are tetrahedrally and octahedrally coordinated with oxygen anions. Note the hydrogen bond between carboxylate and carboxylic group. (b) Monodentate bond of maleic acid with the native oxide according to the adhesive-cluster model No. **5** in Figure 5. The aluminum cation has an octahedral coordination with oxygen anions. The two acid groups are linked by a hydrogen bond. (c) Bridged chelate bond of maleic acid with the native oxide according to the adhesive-cluster model No. **8** in Figure 5. Both aluminum cations are tetrahedrally coordinated with oxygen anions. Here, the acid group is immobilized by a hydrogen bond with the oxide surface.

Downloaded At: 09:21 22 January 2011

lysis is delivered from the top adsorption layer on the oxide surface or from the humidity in the laboratory atmosphere. In addition, we observed a quick evaporation of maleic anhydride. This shows that the maleic anhydride itself does not tend to adhere strongly on the oxide.

The maleic acid molecules are bonded in at least three different ways. The dominating chemical bond corresponds to configuration No. **3** in Figure 4 and is depicted in a more schematic way in Figure 8a.

The acid forms a bridged chelate bond between a carboxylate group and two aluminum cations at the oxide surface. The aluminum ions are tetrahedrally and octahedrally coordinated with oxygen anions, respectively. The second acid group is hampered for polymerization by an intramolecular hydrogen bond with the bonded carboxylate group. Figure 8b illustrates the second kind of chemical adhesion which is provided by a monodendate bond between the carbonyl function of one acid group and one aluminum cation in an octahedral coordination with oxygen (compare also No. **5** in Figure 5). Again, the acid groups

form an intramolecular hydrogen bond. The third type of chemical adhesion consists of a bridged chelate bond of a carboxylate group with two aluminum cations which are both in tetrahedral oxygen coordination. The remaining acid group is immobilized via a hydrogen bond with the oxide surface. The corresponding scheme is given in Figure 8c according to the adhesive-cluster model No. **8** in Figure 5.

The hydrolysis of the anhydride and the subsequent binding of the maleic acid to the oxide by various chemical adhesion mechanisms could result in a distorted epoxy network structure for two reasons. First, it is known from the curing of epoxies with a carboxylic acid in the bulk that the reactivity of such systems is much lower than for the anhydride itself. Second, the acid groups that are not involved in chemical bonds with the substrate are immobilized by various hydrogen bonds. As a consequence, the creation of bonded maleic acid might be considered as a depletion of curing agent in the adhesive mixture in the vicinity of the surface. However, these conclusions have to be checked by further studies because the presence of the oxide surface could change the conditions for the curing reactions in an unexpected and drastic way.

Downloaded At: 09:21 22 January 2011

REFERENCES

[1] Sharpe, L. H., *J. Adhesion* **4**, 5–64 (1972).
[2] Boerio, F. J., Boerio, J. P. and Bozian, R. C., *Appl. Surf. Sci*. **31**, 42–58 (1988).
[3] Brogly, M., Bistac, S. and Schultz, J., *Polym. Int*. **44**, 11–18 (1997).
[4] Holubka, J. W., Dickie, R. A. and Cassatta, J. C., *J. Adhes. Sci. Technol*. **6**, 243–252 (1992).
[5] Drabold, D. A., Adams, J. B., Anderson, D. C. and Kieffer, J., *J. Adhesion* **42**, 55–63 (1993).
[6] Schneider, B., *Doctoral Thesis*, Saarland University, Saarbrücken, Germany, 2001.
[7] Do, N. T. and Baerns, M., *Applied Catalysis* **45**, 9–45 (1988).
[8] Thery, S., Jaquet, D. and Mantel, M., *J. Adhesion* **56**, 1–13 (1996).
[9] Sathyanarayana, D. N. and Savant, V. V., *Z. Anorg. Allg. Chem*. **385**, 239–336 (1971).
[10] Brown, N. M. D., Nelson, W. J. and Walmysley, D. G., *Chem. Soc. Faraday Trans. II* **75**, 32–37 (1979).
[11] Possart, W., Fanter, D., Hartwig, A., Hennemann, O.-D. and Bauer, M., Preprints, *Adhesion European Conference EURADH 94*, Section Francaise de l'Adhesion, Division de la Societe Francaise du Vide–Institute of Materials Adhesives Group U.K.–Dechema e.V. Deutschland, Mulhouse, France, 12–15 September 1994, p. 354.
[12] Possart, W., Fanter, D., Bauer, M., Hartwig, A. and Hennemann, O.-D., *J. Adhesion* **54**, 261–275 (1995).
[13] Valeske, B., Berg, S. and Possart, W., Preprints Poster Presentations, *EURADH '98 4th European Conference on Adhesion and WCARP-1 1st World Congress on Adhesion and Related Phenomena*, Dechema e.V., Fachsektion Klebtechnik, Deutschland, Société Française d'Adhésion, The Institute of Materials UK, The

Adhesion Society USA, The Adhesion Society of Japan, Garmisch-Partenkirchen, Germany, 6–11 September 1998, No. 1.16.
[14] Wefers, K. and Misra, C., *Alcoa Technical Paper* No. 19, Alcoa, (1987).
[15] De Laet, J., Vanhellemont, J., Terryn, H. and Vereecken, J., *J. Appl. Phys. A* **54**, 72–78 (1992).
[16] Jimenez-Gonzalez, A. and Schmeisser, D., *Surf. Sci.* **250**, 59–70 (1991).
[17] Graedel, T. E., *J. Electrochem. Soc.* **136**, C204–C212 (1989).
[18] Thomas, P. V., Ramakrishnan, V. and Vaidyan, V. K., *Thin Solid Films* **170**, 35–40 (1989).
[19] Lee, M.-H., Cheng, C.-F., Heine, V. and Klinkowski, J., *Chem. Phys. Lett.* **265**, 673–676 (1997).
[20] El-Mashri, S. M., Forty, A. J., Freeman, L. A. and Smith, D. J., *Electron Microscopy and Analysis*, p. 395–398 (1981).
[21] Norman, D., Brennan, S., Joeger, R. and Stohr, J., *J. Surf. Sci.* **105**, L297–306 (1981).
[22] Barna, P. B., Bodo, Z., Gergely, G., Croce, P. and Jakab, P., *Thin Solid Films* **110**, 249–256 (1984).
[23] Volpe, L., *Key Eng. Mater.*, 20–28, 4091–4097 (1988).
[24] Peri, J. B., *J. Phys. Chem.* **69**, 220–230 (1965).
[25] Alcock, N. W., Tracy, V. M. and Waddington, T. W., *J. Chem. Soc. Dalton*, 2243–2246 (1976).
[26] Bérces, A. and Ziegler, T., In: *Density Functional Theory III, Topics in Current Chemistry*, Dunitz, J. D., Hafner, K., Houk, K. N., Ito, S., Lehn, J.-M., Raymond, K. N., Rees, C. W., Thiem, J. and Vögtle, F., Eds., vol. 182 (Springer, Berlin, 1996), pp. 41–85.
[27] Wong, M. W., *Chem. Phys. Lett.* **256**, 391–399 (1996).
[28] Andzelm, J. and Wimmer, E., *J. Chem. Phys.* **96**, 1280–1303 (1992).
[29] Seminario, J. M. and Politzer, P., Eds., *Modern Density Functional Theory: A Tool for Chemistry* (Elsevier, Amsterdam, 1995).
[30] Schneider, B. and Possart, W., *Proceedings of the 24th Annual Meeting of the Adhesion Society "Adhesion Science for the 21st Century,"* Williamsburg, VA, USA, 25–28 February 2001, p. 236–238.

Downloaded At: 09:21 22 January 2011